Quasiperiodic one-dimensional photonic crystals with adjustable multiple photonic band gaps

ANDREY M. VYUNISHEV[1,2,*], PAVEL S. PANKIN[2,3], SERGEY E. SVYAKHOVSKIY[4], IVAN V. TIMOFEEV[1,3], AND STEPAN YA. VETROV[1,2]

[1]*Kirensky Institute of Physics, Federal Research Center KSC SB RAS, Krasnoyarsk, 660036, Russia*
[2]*Institute of Engineering Physics and Radio Electronics, Siberian Federal University, Krasnoyarsk, 660041, Russia*
[3]*Institute of Nanotechnology, Spectroscopy and Quantum Chemistry, Siberian Federal University, Krasnoyarsk 660041, Russia*
[4]*Department of Physics, M.V. Lomonosov Moscow State University, Moscow, 119991, Russia*
[*]*Corresponding author: vyunishev@iph.krasn.ru*

Compiled August 17, 2017

We propose an elegant approach to produce photonic band gap structures with multiple photonic band gaps (PBGs) by constructing quasiperiodic photonic crystals (QPPCs) composed by a superposition of photonic lattices with different periods. Generally QPPC structures exhibit both aperiodicity and multiple PBGs due to their long-range order. They are described by a simple analytical expression instead of quasiperiodic tiling approaches based on substitution rules. Here we describe the optical properties of quasiperiodic photonic crystals exhibiting two PBGs that can be tuned independently. PBG interband spacing and their depths can be varied by choosing appropriate reciprocal lattice vectors and their amplitudes. These effects are confirmed by the proof-of-concept measurements made for the porous silicon based QPPC of the appropriate design.

OCIS codes: *(230.5298) Photonic crystals; (290.4210) Multiple scattering; (350.2460) Filters, interference.*

http://dx.doi.org/10.1364/ao.XX.XXXXXX

Photonic crystals (PC) have attracted much attention in the last decades since the concept was introduced [1]. The main feature of PCs is the existence of photonic band gap (PBG) with prohibited transmission [1, 2]. Insertion of a defect layer into PCs breaks the periodicity and results in the appearance of a defect mode placed within the PBG, which can be used for spectral filtering. Depending on their composition, PCs can conditionally be distinguished as periodic, quasiperiodic and aperiodic photonic crystals. There are common ways for the formation of quasiperiodic photonic crystals (QPPCs), which are also called as deterministic aperiodic structures [3] or tilings, and that are the intermediate between the periodic and aperiodic PCs. Some substitution rule representing a mathematical sequence in layer positions has to be introduced to interleave layers with different refractive indexes to form a QPPC structure. So far, QPPCs of several kinds have been investigated; among them are Fibonacci, Thue-Morse, Rudin-Shapiro, double periodic, octonacci, Cantor and Pell-like structures [4]. Earlier, deterministic PCs were successfully used for optical filtering, multi-frequency terahertz manipulation, near-perfect absorption and omnidirectional reflection, photoluminescence emission enhancement [5–12]. Fibonacci and Thue-Morse-like photonic structures have been reported for the Bloch-like surface waves [13] and multimode photon-exciton coupling [14], which represent a significant advantage compared to periodic PC counterparts. Alternatively, introduction of random deviations into the layer thicknesses or refractive indexes violates the periodicity of a structure thus leading to widening of photonic band gaps [15–17]. Another kind of 1D PC structures represents a logical combination of two 1D PCs of close periods [18]. The transmission spectrum of these structures demonstrates the frequency region with a finite number of slow modes. Recently, Alagappan et al. considered a dual-periodic structure obtained by summation of the two harmonic functions [19]. Such structures can be used for designing high quality, broadband and multichannel slow light devices to create a new class of passive superluminal structures. Nevertheless the formation of deterministic PC structures with required optical characteristics are complicated and secondary (parasitic) PBGs may appear.

In this letter, we propose a way for the composition of quasiperiodic photonic crystals with pre-designed multiple photonic band gaps. The QPPC is constructed by a superposition of several spatial harmonics with different spatial frequencies, that determine the spectral position of multiple PBGs. We show that the spectra of such QPPCs represent a combination of those for the two conjugated periodic 1D PCs. To the best of our knowledge, such an approach has not been applied for the composition of linear PCs, while it was considered in nonlinear optics for the multi-wavelength conversion [20, 21] and multiple spatial harmonic generation [22].

The refractive index of the proposed linear QPPC structure

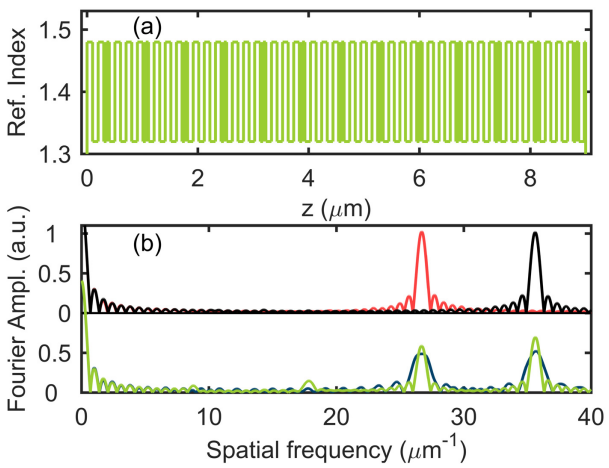

Fig. 1. (a) Modulation of the refractive index calculated using Eq. (2), and (b) Fourier transform of the refractive index as a function of spatial coordinate for both periodic PC (red and black), for conjugated PCs (indigo) and QPPC (yellow green) structures.

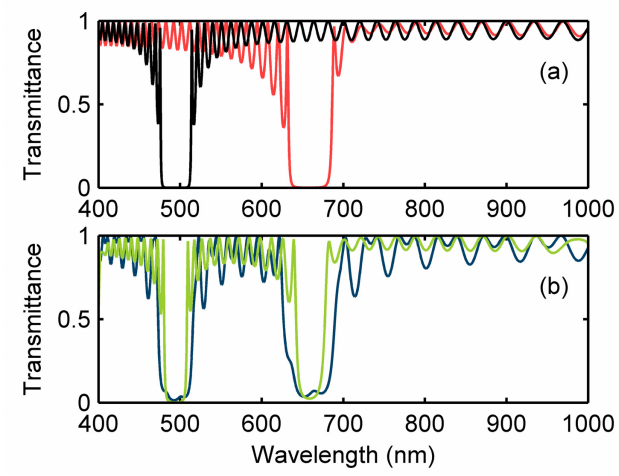

Fig. 2. (a) Calculated transmission spectral dependencies for periodic PC with $|\mathbf{G}_1|$ = 26.7 rad $\cdot\mu$m^{-1} (red) and $|\mathbf{G}_2|$ = 35.6 rad $\cdot\mu$m^{-1} (black). (b) Calculated transmission spectra for the conjugated PCs (indigo) and QPPC (yellow green).

is described by

$$n(z) = n_0 + \Delta n \mathrm{sgn}\left(\sum a_j \sin\left[\mathbf{G}_j z + \phi_j\right]\right). \quad \textbf{(1)}$$

Here n_0 is the average refractive index, Δn is the maximum deviation of the refractive index from its average value n_0, a_j, $\mathbf{G}_j$ and ϕ_j are the amplitude, reciprocal lattice vector (RLV) and relative phase of the j^{th} spatial harmonic, $\mathrm{sgn}(x) = |x|/x$ is a signum function. We restrict our consideration by the case of two RLVs, so that Eq. (1) is simplified to

$$n(z) = n_0 + \Delta n \mathrm{sgn}\left(a_1 \sin \mathbf{G}_1 z + a_2 \sin \mathbf{G}_2 z\right). \quad \textbf{(2)}$$

We study the spatial and spectral characteristics of QPPC in comparison to the 1D PC with $\mathbf{G}_1$ and $\mathbf{G}_2$. In the plane wave approximation and for the linearly polarized waves, the wave propagation in arbitrary structured PC and respective transmission coefficients can be calculated using the transfer-matrix formalism [23]. Modulation of the refractive index becomes a periodic one if any of two amplitudes in Eq. (2) equals to zero ($a_2 = 0$). The period of the structure is $\Lambda = 2\pi/|\mathbf{G_1}|$, and its Fourier transformation demonstrates a maximum at the spatial frequency G_1 (Fig. 1(b)). As a result, the first order PBG in the transmission spectrum appears that corresponds to the RLV G_1 (Fig. 2(a)), which spectral position satisfies the Bragg condition [1, 2]:

$$\lambda_m = 2\pi(n_1 + n_2)/mG, \quad \textbf{(3)}$$

where $n_{1,2}$ are the refractive indexes of the PC constituting layers.

Keeping both terms in Eq. (2), we get a more complicated spatial modulation of the refractive index corresponding to the QPPC structure (Fig. 1(a)). In our calculation we used the parameters that were taken for the fabrication of the porous silicon QPPC described below. So we took: $n_0 = 1.40$, $\Delta n = 0.08$, $a_1 = a_2$, $|\mathbf{G}_1| = 26.7$ rad $\cdot\mu$m^{-1}, $|\mathbf{G}_2| = 35.6$ rad $\cdot\mu$m^{-1}. The period of QPPC structure is $\Lambda = 2\pi/|\mathbf{G_3}|$, where $|\mathbf{G}_3| = G_3$ is a highest common factor of $\{G_1, G_2\}$. If G_2/G_1 is a rational number then Λ is a finite number and the structure possesses the translational symmetry. In the case under study, the highest common factor G_3 is 8.9 rad $\cdot\mu$m^{-1}. Then the period of QPPC equals to 0.706 μm, and 12 periods fall on the thickness of QPPC. The QPPC period contains 8 layers in a unit cell. Such a structure differs from common 1D photonic crystals based on bilayer structures or even of a more specific case of three-layered structures described previously (see, e.g. [24, 25]). In our case, the proper choice of RLVs can provide the unit cell consisting of arbitrary number of layers, therefore the unit cell may exceed an overall thickness of the structure. The Fourier spectrum of the structure described by Eq. (2) demonstrates the presence of two peaks corresponding to the spatial frequencies G_1 and G_2, instead of one at G_3 arising from the periodicity of QPPC structure (Fig. 1(b)). Accounting for an interplay between the spatial and spectral characteristics, we expect the appearance of the two PBGs with the spectral positions defined by Eq. (3). Indeed, the calculated transmission spectrum of the QPPC confirms this assumption (Fig. 2(b)): one can see the presence of two PBGs with the central wavelength corresponding to that of periodic PCs as is shown in Fig. 2(a). In general, the PBG central wavelengths can be found from Eq. (3) by substituting the values G_1 and G_2. In this case the ratio of G_1 to G_2 is 3:4 and the PBG central wavelengths are given by G_3 with multipliers $m = 3$ and 4, respectively. Our calculations demonstrate that optical waves undergo the selective Bragg diffraction for both RLVs. Note that the approach provides the Fourier amplitudes for relevant RLVs as high as possible, which is evident from the comparison of the QPPC and the two conjugated PCs shown in Fig. 1(b)). It makes QPPCs differing from other deterministic PCs (see, e.g.[5–12]), where series of parasitic PBGs are exhibited.

Compare QPPC with more straightforward implementation of PC stacked by two conjugated periodic PCs with the primary spatial frequencies $G_{1,2}$. Fig. 2(b) shows calculated transmission spectra for QPPC and for the conjugated PC stacked by two 4.5-μm-thick periodic PCs. For the conjugated PCs the edges and the bottom of the PBGs suffer from distortions, while QPPC provides PBGs with smooth and sharp edges. Moreover, average interband transmittance of QPPC manifestates weaker

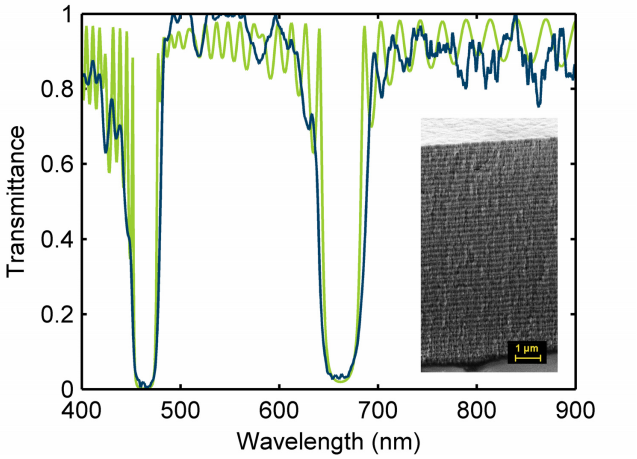

Fig. 3. Measured (indigo) and calculated (yellow green) transmission spectral dependence of QPPC with G_1 = 26.7 rad $\cdot\mu$m^{-1} and G_2 = 35.6 rad $\cdot\mu$m^{-1}. Insertion: SEM image of the porous silicon-based QPPC structure (Sample 5 from Table 1).

Table 1. Predesigned and Fitted values of RLV $\mathbf{G}_2$ as well as Measured and Calculated (Eq. (3)) PBG central wavelengths at fixed G_1 = 26.7 rad $\cdot\mu$m^{-1}

Sample #	Predesigned $\mathbf{G}_2$ (rad $\cdot\mu$m^{-1})	Fitted $\mathbf{G}_2$ (rad $\cdot\mu$m^{-1})	$\lambda_{meas.}$ (nm)	$\lambda_{calc.}$ (nm)
1	17.8	18.1	976	972
2	22.2	22.4	790	785
3	26.7	26.8	655	657
4	31.1	30.9	570	570
5	35.6	37.9	464	464
6	40.0	44.3	398	397

oscillations. The same difference is deduced from the analysis of the Fourier spectra of both structures (Fig. 1(b)).

For the proof-of-concept experiments, the QPPC based on mesoporous silicon is fabricated by electrochemical etching of crystalline silicon [26]. The refractive indexes of the layers were 1.32 and 1.48, providing $n_0 = 1.40$, $\Delta n = 0.08$. The structure has the thickness 9 μm and contains 52 layers. As shown in Fig. 3, the measured QPPC transmission spectra demonstrate two PBGs centered at 494 and 660 nm, respectively. The refractive indexes and primary RLV were reasonably tuned to obtain a good agreement between calculated and measured transmission spectra. The designed and fitted values of G_2 are given in Table 1. The adjustment of these values is imposed by the uncertainty inherent to the sophisticated fabrication method of QPPC. Nevertheless, it can be deduced that the proper choice of RLVs can fit the transmittance dependencies of QPPC. In addition, by varying the amplitudes a_j in Eq. (1) we can distribute the ratio of transmittance or reflectance between the individual PBGs.

In order to reveal the dependence of the transmission spectra on the continuous variation of the ratio of $\mathbf{G}_1$ and $\mathbf{G}_2$, we made a set of structures with the fixed $\mathbf{G}_1$ and varied $\mathbf{G}_2$ values.

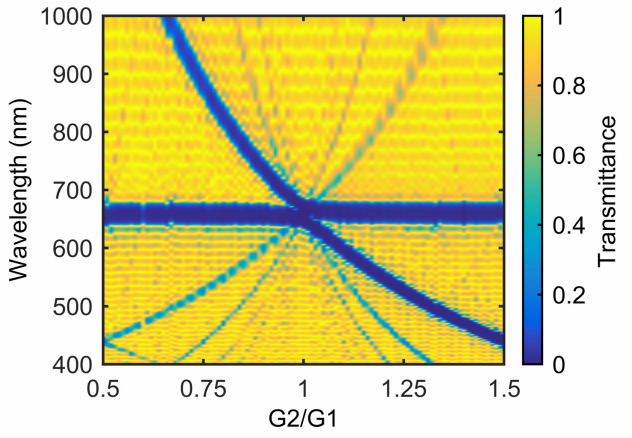

Fig. 4. Calculated transmission spectral dependence of QPPC versus the fraction $\mathbf{G}_2$ / $\mathbf{G}_1$.

The PBG corresponding to $\mathbf{G}_2$ shifts towards short wavelengths while increasing the value of $\mathbf{G}_2$ (Fig. 4). The PBG for $\mathbf{G}_1$ keeps its position except for a small spectral shift in the vicinity of PBG crossing point at $|\mathbf{G}_2| = |\mathbf{G}_1|$, corresponding to the single periodic PC. The adjustment of the spatial frequencies $\mathbf{G}_1$ and $\mathbf{G}_2$ is used to form the pass band with arbitrary width in the visible spectral range. Moreover, a set of additional narrow PBGs appear inside the pass bands. It can be seen that these PBGs are equidistant in the frequency domain and correspond to the Fourier transform peaks of Fig. 1(b) with the spatial frequency increment G_3. They originate from a nonharmonic spatial profile of the dielectric permittivity and are well evaluated using the coupled mode theory (see Ch.12 of [27]). These PBGs represent the mirror counter-part of the primary PBGs in the frequency domain.

Fig. 5 shows the measured transmittance spectra for all QPPC samples *vs* the value of G_2. It is clearly seen that the PBG corresponding to G_2 exhibits a pronounced spectral shift. The experimental results are in a good agreement with the numerical results shown in Fig. 4. The experimental and theoretical results are summarized in Table 1. As one can see, the fitted values G_2 are close enough to the predesigned values, as well as the PBG central wavelengths calculated for fitted RLV G_2 are in the vicinity of the measured values.

The analysis of the transmission and reflectance spectra allowed to estimate the attenuation of the sample by 1.2 cm^{-1} at 670. This value is higher than the absorption of amorphous quartz. This discrepancy can be explained by the light scattering on the layer interfaces.

Summing up, we propose a versatile approach of refractive index superposition modulation for structuring quasiperiodic photonic crystals with adjustable multiple band gaps. The obtained results show that the light undergoes the selective Bragg diffraction resulting from a long-range order of QPPC. PBGs spectral position and their depths can be specified prior to the fabrication by a proper choice of RLVs. The approach proposed can be extended to a wide range of wave phenomena of arbitrary nature in periodic structures in such areas as acousto-optics, plasmonics and magnonics.

Russian Foundation for Basic Research (RFBR) and Government of Krasnoyarsk Territory, Krasnoyarsk Region

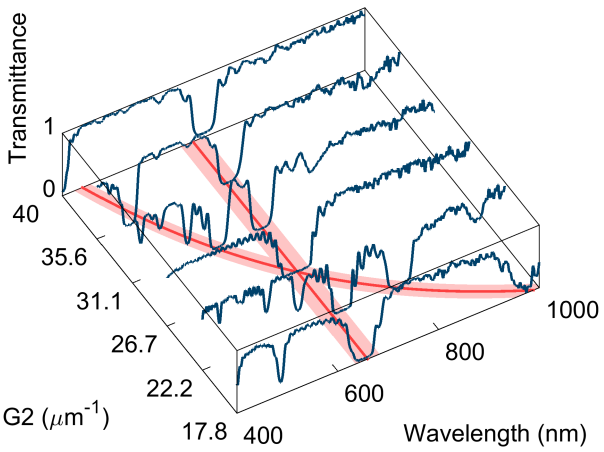

Fig. 5. Measured transmission spectra of QPPC (indigo) on the value $\mathbf{G}_2$ and corresponding PBG central wavelength positions calculated by using Eq. (3) (red).

Science and Technology Support Fund (16-42-243065); RFBR (16-02-01100); Scholarship of the President of the Russian Federation (SP-3372.2015.5, SP-227.2016.5).

The authors thank Prof. T.V. Murzina, M.Y. Shalaginov and Prof. V.M. Shalaev for help and fruitful discussions.

REFERENCES

1. E. Yablonovitch, Phys. Rev. Lett. **58**, 2059 (1987).
2. J. D. Joannopoulos, S. G. Johnson, J. N. Winn, and R. D. Meade, *Photonic Crystals: Molding the Flow of Light* (Princeton University Press, 2011).
3. L. Dal Negro, *Optics of aperiodic structures: fundamentals and device applications* (CRC Press, 2013).
4. Z. V. Vardeny, A. Nahata, and A. Agrawal, Nat. Photon. **7**, 177 (2013).
5. M.S. Vasconcelos, P.W. Mauriz, and E.l. Albuquerque, Microelectronics Journal **40**, 851 (2009).
6. Y. Qin, C. Zhang, D. Zhu, Y. Zhu, H. Guo, G. You, and S. Tang, Optics express **17**, 11558 (2009).
7. Y. Gong, X. Liu, L. Wang, H. Lu, and G. Wang, Opt. Express **19**, 9759 (2011).
8. H.-F.Zhang, J.-P. Zhen, and W.-P.He, Optik **124**, 4182 (2013).
9. E.R. Brandao, C. H. Costa, M.S. Vasconcelos, D.H.A.L. Anselmo, and V.D. Mello, Optical Materials **46**, 378 (2015).
10. J. Da, Q. Mo, Y. Cheng, and T. Liu, Physica B: Condensed Matter **458**, 63 (2015).
11. D. Lusk, I. Abdulhalim, and F. Placido, Opt. Commun. **198**, 273 (2001).
12. J. Hendrickson, B. C. Richards, J. Sweet, G. Khitrova, A. N. Poddubny, E. L. Ivchenko, M. Wegener, and H. M. Gibbs, Opt. Express **16**, 15382 (2008).
13. V. Koju and W. M. Robertson, Opt. Lett. **41**, 2915 (2016).
14. K. Zhang, Y. Xu, T.-Y. Chen, H. Jing, W.-B. Shi, B. Xiong, R.-W. Peng, and M. Wang, Opt. Lett. **41**, 5740 (2016).
15. D. Zhang, Y. Zhang, W. Hu, Z. Li, and B. Cheng, Appl. Phys. Lett. **67**, 2431 (1995).
16. D. Zhang, W. Hu, Y. Zhang, Z. Li, B. Cheng, and G. Yang, Phys. Rev. B **50**, 9810 (1994).
17. H. Li, H. Chen, and X. Qiu, Physica B: Condensed Matter **279**, 164 (2000).
18. G. Alagappan and C.E. Png, Nanoscale **7**, 1333 (2015).
19. G. Alagappan and C.E. Png, Sci. Rep. **6**, 1 (2016).
20. T. W. Ren, J. L. He, C. Zhang, S. N. Zhu, Y. Y. Zhu, and Y. Hang, J. Phys.: Cond. Matt. **16**, 3289 (2004).
21. A. A. Novikov and A. S. Chirkin, J. Exp. Theor. Phys. **106**, 415 (2008).
22. A. M. Vyunishev and A. S. Chirkin, Opt. Lett. **40**, 1314 (2015).
23. P. Yeh, A. Yariv, and C.-S. Hong, J. Opt. Soc. Am. **67**, 423 (1977).
24. Y. Zhang and Q. Wang, Optoelectron. Lett. **2**, 44 (2006).
25. A. Baldycheva, V. A. Tolmachev, T. S. Perova, Y. A. Zharova, E. V. Astrova, and K. Berwick, Opt. Lett. **36**, 1854 (2011)
26. S. E. Svyakhovskiy, A. I. Maydykovsky and T. V. Murzina, J. Appl. Phys. **112**, 013106 (2012).
27. A. Yariv and P. Yeh, *Photonics: Optical Electronics in Modern Communications*, The Oxford Series in Electrical and Computer Engineering (Oxford University Press, 2007).